Film thickness effects on mechanical and tribological properties of nitrogenated diamond-like carbon films

Jun Qi[a,b], C.Y. Chan[a], I. Bello[a], C.S. Lee[a], S.T. Lee[a,*], J.B. Luo[b], S.Z. Wen[b]

[a]Center Of Super-Diamond & Advanced Films (COSDAF) and Department of Physics and Materials Science, City University of Hong Kong, Hong Kong, PR China
[b]State Key Laboratory of Tribology, Tsinghua University, Beijing 100084, PR China

Abstract

Nanoindentation, nanoscratch and ball-on-disk tests were used to determine the film thickness effect on the mechanical and tribological properties of nitrogenated diamond-like carbon (CN_x) films, which were deposited on Si (100) substrates by an electron cyclotron resonance microwave plasma chemical vapor deposition (ECR MP-CVD) system. Except for the film with a thickness of 20 nm, there existed peak values of hardness for all films thicker than 44 nm. When the thickness ranged from 44 to 235 nm, the peak values of hardness and the corresponding indentation depth increased along with increasing film thickness. The results of scratch resistance tests showed that the critical loads of the fracture were independent of thickness for thinner films, however, they increased rapidly with increasing thickness for thicker films. Ball-on-disk sliding tests indicated that the friction coefficient decreased with increasing thickness for thinner films, while there was no obvious thickness dependence of the friction coefficient for relatively thicker films. The formation of transferred layer and graphitization of the films during sliding resulted in the decrease of friction coefficients at early stages of sliding. © 2001 Elsevier Science B.V. All rights reserved.

Keywords: Nitrogenated diamond-like carbon; Mechanical properties; Tribology

1. Introduction

Hard films have been widely used as protective coatings to enhance hardness and wear-resistance ability of bulk materials surfaces. Among many hard coatings, diamond-like carbon (DLC) films have received considerable interest over the past two decades because of their high hardness, wear resistance, as well as attractive optical and electrical properties [1,2]. These excellent properties constitute the DLC films for many applications in industrial fields, including magnetic hard disk, forming instruments and even cutting tools. However, their high compressive stress is the main limitation in many applications. Arora et al. [3] discussed the problem of high compressive stress and its relaxation. They demonstrated that nitrogen incorporation in DLC films could lower the high compressive stress but would not affect significantly other desired properties. Hence, nitrogenated diamond-like carbon (CN_x) films have become very competitive with DLC films in many applications.

It is well known that to design engineers, it is vital to consider the selection of film thickness in mechanical and tribological applications. Several experimental investigations have shown that the coating thickness is a key parameter to prolong the lifetime in rolling contacts by using hard coatings [4,5]. Wang et al. [6]

* Corresponding author. Tel.: +852-2788-7831; fax: +852-2784-4696.
E-mail address: apannale@cityu.edu.hk (S.T. Lee).

showed that the coating thickness of carbon nitride film had some effects on the surface damage during sliding contact. Although the film thickness is a key factor in product quality, the thicker films do not necessarily render the higher performance of coated products. Therefore, the film thickness should be optimized for both performance and cost effectiveness as the thinner films may perform well at lower production cost. Many researchers have studied the mechanical and tribological properties of CN_x films [7–11], however, there have been only very few reports related to the effect of thickness [12] on the properties of CN_x films [4–6].

In the present work, we employed nanoindentation, nanoscratch and ball-on-disk testings to determine the thickness effects on the mechanical and tribological properties of CN_x films prepared by electron cyclotron resonance microwave plasma chemical vapor deposition (ECR MP-CVD).

2. Experimental

An Astex ECR-MPCVD system, described elsewhere [13], was used to deposit CN_x films. Briefly, microwave power of 2.45 GHz from a 5-kW microwave power generator was introduced into the plasma generation chamber. By applying an electrical current of 180 A to a magnetic coil, a magnetic field of 875 G was generated. This magnetic induction satisfies the ECR conditions in the plasma chamber. The samples were loaded on a graphite holder and radio frequency biased at 13.6 MHz. Si (100) wafers were used as substrates and cleaned ultrasonically in acetone and ethanol baths before introducing them into a deposition chamber. The base pressure in the ECR deposition chamber was lower than 2×10^{-4} Pa. Prior to deposition the substrates were sputter-cleaned for 10 min in argon plasma at -120 V substrate bias voltage. During deposition, the microwave power and substrate voltage were preset to 500 W and -120 V, respectively. The flow rates of argon, acetylene and nitrogen were kept constant at 60, 3 and 2 sccm, respectively, during films deposition. The thickness of the CN_x films prepared on Si substrates was determined by a surface profiler.

The hardness and elastic modulus of the film/substrate systems were measured by a Nano Indenter XP system. Nanoindentation measurements were carried out using a continuous stiffness measurement (CSM) technique enabling the measurement of hardness and elastic modulus as functions of indentation depth. The analysis of nanoindentation data followed the approach of Oliver and Pharr [14]. The Nano Indenter XP system was also used for the nanoscratch tests of the films. In the nanoscratch tests, one edge of the diamond tip was aligned with the scratch direction. During scratching, a ramp load was applied over a length of 500 μm until

reaching a preset normal load of 40 mN. Each representative value in both nanoindentation and nanoscratch tests was the average value obtained from five individual tests in different parts of the sample. The morphologies of scratch scars were observed with an optical microscope.

The dry sliding friction characteristics of the CN_x films at room temperature were evaluated using a CSEM ball-on-disk tribometer. A Si_3N_4 ball with 6 mm in diameter was balanced on the CN_x films surface and loaded with 1 N. In all experiments, the sliding speed was 3 cm/s. During measurement, the relative humidity was $50 \pm 3\%$. The morphologies of wear tracks of the ball and the CN_x films were observed with an optical microscope.

3. Results and discussion

3.1. Hardness and modulus

Fig. 1a,b show the hardness and elastic modulus of the CN_x films as functions of indentation depth, respectively. As a comparison, the hardness and elastic modulus of bare Si (100) substrate are drawn out in open circles. Fig. 1a indicates that for the thickness of 20 nm the trend of the hardness was very similar to that of the bare silicon substrate. The hardness first increased with increasing indentation depth and then remained constant all the way. For films with thickness above 44 nm peak values of the hardness were identified. The hardness first increased with increasing indentation depth to a maximum beyond which the hardness continuously reduced until reaching the hardness of the silicon substrate. Furthermore, for films with thickness in the 44- and 235-nm range, the peak values of the hardness and the corresponding indentation depth increased with increasing thickness of CN_x films. Above the thickness of 235 nm, the peak value of hardness did not increase any more though there was still some increase in indentation depth. Despite the large differences in the hardness at different film thickness, the elastic modulus of the same series of samples, as shown in Fig. 1b, was very similar within the experimental error range.

In the hardness testing of the film/substrate system using nanoindentation technique, the deformation in the film was determined by both the film itself and substrate. Therefore, the measured hardness value was a composite one. The load-support capacity of a very thin film was low and the deformation during indentation was mainly determined by the substrate. Hence, when the film was very thin, the measured hardness would be similar to that of the substrate. The thicker film would carry a larger portion of the load and consequently the deformation in the substrate would
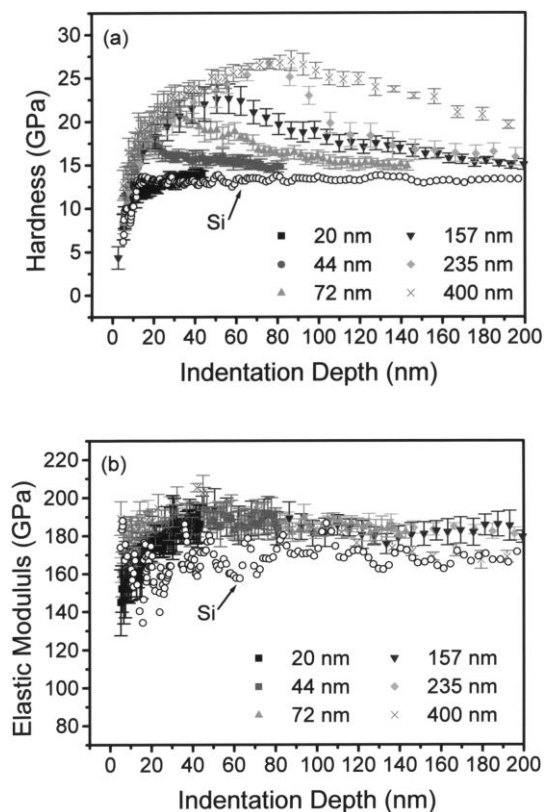
Fig. 1. Hardness (a) and elastic modulus (b) as functions of the indentation depth for CN$_x$ films with different thickness. For reference, the hardness and elastic modulus of a bare Si (100) substrate are plotted using open circles.

be smaller. Thus, reducing the substrate effect led to a higher hardness value. During indentation, the substrate supported the film and the film would bend to conform to the substrate deformation. If plastic deformation occurred in the substrate, a part of the load-support capacity of the substrate would be lost, which may result in the decrease of hardness after reaching the maximum value. Thus, for thicker films a larger indentation depth is required for occurring plastic deformation in the substrate. Therefore, the indentation depth corresponding to the peak values of the hardness increased with increasing thickness of CN$_x$ films. Two main reasons can attribute to the similarity of the elastic modulus at different film thickness. Firstly, the difference between the elastic modulus of the films and substrate was not as large as that between the hardness, thus the substrate influence on the elastic modulus was not significant. In contrast to the elastic modulus, which is an intrinsic material property, the hardness is effected not only by the tested sample but also external factors, and therefore it is sensitive to the test conditions. The elastic modulus did not vary so much as the hardness with the increase in film thickness.

Since the peak values of the hardness above a thickness of 235 nm did not vary much, we thought these

maximum hardness values were more representative in describing the films than those for thinner films. It should be noted that all indentation depths giving rise to the peak values of the hardness exceeded one-tenth of the corresponding film thickness. Although the well-known rule in hardness testing is that the indentation depth should not exceed one-tenth of the film thickness at which the contribution of the substrate can be negligible, some researchers demonstrated that this was not a general rule [15,16]. For microindentation hardness testing the critical ratio of depth to thickness, at which the contribution of the substrate is negligible, varied sensitively with coated systems [17]. Therefore, particular attention should be paid in hardness testing of coated systems when using the nanoindentation technique.

3.2. Scratch resistance test

Fig. 2 shows the representative optical micrographs of the scratch tracks made on the CN$_x$ films with different thickness. As shown in Fig. 2, the coating fracture occurred at the end stage of scratching while the residual plastic deformation on the film surface was induced before approaching the initial point of fracture. When the film thickness was low, there was no obvious spalling on both sides of the scratch track. At high film thickness, spalling along the scratch track became more serious. From the initial points of fracture in the scratch tracks combined with the preset load before scratching, the normal load associated with the initial fracture of the films, which was defined as the critical load of film fracture, could be obtained. The critical load of film fracture for the CN$_x$ films as a function of the film thickness is shown in Fig. 3. In the low film thickness region, the film thickness had no significant effect on the critical load. Afterwards, the critical load increased rapidly with increasing film thickness. However, when the film reached 250 nm, the increase rate in critical load slowed down.
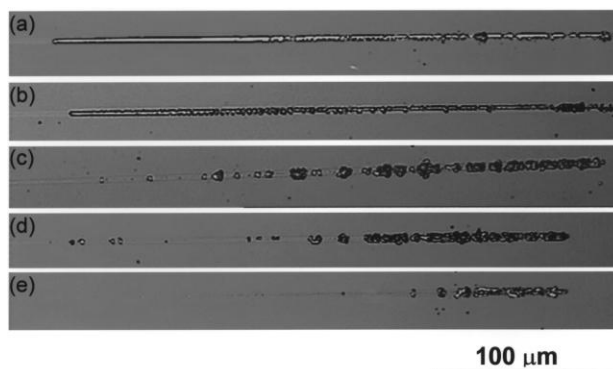
Fig. 2. Representative optical micrographs of scratch tracks made on CN$_x$ films with different thickness: (a) 72 nm; (b) 100 nm; (c) 157 nm; (d) 235 nm; and (e) 400 nm.
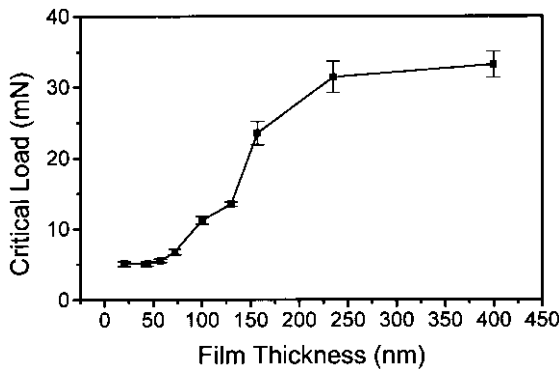
Fig. 3. Critical load of film fracture during scratching as a function of film thickness for CN_x films with different thickness.

Fig. 4. Variation of friction coefficients as a function of the sliding distance for the CN_x films with different thickness.

The indenter has two simultaneous directional movements during scratching. One is the normal indentation process and the other is the horizontal motion. From the previous results [18,19], the coating detachment, in scratch test, is induced by: (i) the elastic-plastic indentation stress; (ii) the tangential friction force; and (iii) the inherent internal stress. However, it is argued that the cross-sectional area of the scratch tracks is much smaller than the contact area between the tip and sample [20], therefore the tangential friction force is not expected to play an important role as the other two factors do in the coating removal. In the case of thin films, the plastic deformation may first develop in the substrate due to the indentation stress during scratching since the film was much harder than the substrate. The plastic flow in the substrate easily induced through cracks in the films ahead of the indenter. Therefore, the effect of substrate was more significant than that of the film thickness, and the critical load was almost independent of the film thickness. The lower compressive stress in the thinner films led to less serious spalling along the scratch tracks. With increasing film thickness, the substrate effect would be less under the same load during scratching, which resulted in the increase of the critical load. However, the compressive stress affecting the film adhesion, accumulated with the increase in film thickness. The thicker films tended to delaminate readily and hence the increase rate of the critical load slowed down. It should be noted that the increase of the critical load with increasing film thickness was the feature of the bulk failure mode and did not represent the increase in adhesion between the film and substrate [21].

3.3. Tribological properties

Fig. 4 shows the variation of friction coefficients for the CN_x films with different thickness against the sliding distance. The friction coefficient for a film thickness of 20 nm was very high and fluctuated dramati-

cally. This behavior was similar to that of an uncoated silicon worn by a silicon nitride (Si_3N_4) ball. Except for the film with a thickness of 20 nm, the friction coefficients for other films ranged from 0.1 to 0.3, and at the beginning stage of friction they decreased gradually with increasing sliding distance. Furthermore, the friction coefficient decreased with increasing film thickness for thinner films, while there was no obvious thickness dependence of the friction coefficient for thicker films. The optical micrographs in Fig. 5 show the wear tracks on the CN_x films with different thickness after sliding 0.3 km. Evidently, the widths of the wear tracks on the thinner films were larger than those on the thicker films.
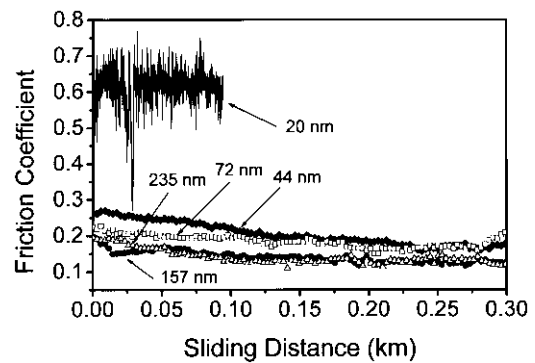
When a hard ball slid over a soft substrate coated by a hard coating, the substrate deformation induced by the normal load and friction force would affect the friction and wear properties of the hard coating. When the film thickness is only 20 nm, the deformation of the substrate must be very large due to the poor load-support capacity of the film and the film would deflect in accordance with the deformation of the substrate. The
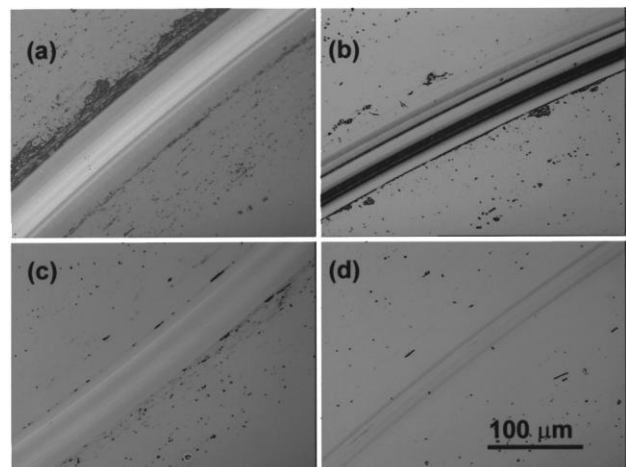
Fig. 5. Representative optical micrographs of wear tracks on the CN_x films with different thickness after sliding 0.3 km: (a) 72 nm; (b) 100 nm; (c) 157 nm; and (d) 235 nm.
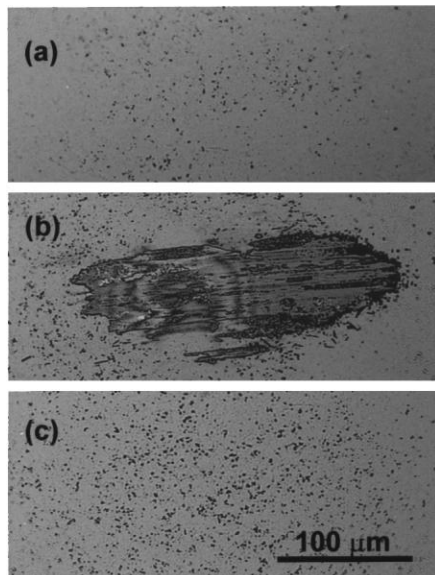
Fig. 6. Optical micrographs of the contact area of the same Si_3N_4 ball before test (a), after sliding 0.3 km over the surface of a CN_x film with a thickness of 157 nm without any cleaning (b) and after rubbed cleaning with a soft paper wetted with ethanol (c).

considerable deformation of the substrate would thus add either a ploughing or hysteresis effect to friction. The repeated deflection of the film might cause fracture or fatigue cracks that destroy the coating or the substrate [22]. Therefore, a very thin film could hardly protect the substrate from destroying during the sliding of a hard Si_3N_4 ball over its surface. The increase of the film thickness led to the reduction of the substrate deformation and hence the contact area between the film and sliding ball. Moreover, thicker films prevented ploughing the substrate more efficiently. The lower contact area combined with less ploughing resulted in the narrower wear tracks and lower friction coefficients for the thicker films. When the film thickness was relatively larger, the effect of the substrate deformation on the friction coefficient under a given load could be negligible because of the high load-support capacity of the film itself. In this case, the friction coefficient would not be strongly dependent on the film thickness. The decrease of the friction coefficient with increasing sliding distance at the beginning of friction could be attributed to the formation of a transferred layer and graphitization of films in the top surface region during sliding. Fig. 6 shows the optical micrographs of the contact area of the same Si_3N_4 ball before test, after sliding 0.3 km over the surface of CN_x film with a thickness of 157 nm with no cleaning (Fig. 6b) and after cleaning (Fig. 6c) using a piece of soft paper dipped with ethanol. As shown in Fig. 6, a transferred layer formed on the Si_3N_4 ball surface after the sliding test, however, it was easily removed by a simple cleaning.

There was no obvious wear scar left on the Si_3N_4 ball surface. This soft transferred film prevented the direct contact between the original materials of ball and the film, and in addition, it reduced the stress concentration on the contact area [23]. On the other hand, it can be easily demonstrated that the G-peak of the Raman spectrum collected from the wear track gave rise to a shift of approximately 2 cm^{-1} towards the higher wavenumber compared to the peak position before the friction testing. Therefore, it is reasonable to consider that the graphitization of the top surface regions of films induced by the released heat during friction process was the reason for reducing the friction coefficient with increasing sliding distance.

4. Conclusions

The thickness of CN_x films, deposited by ECR MP-CVD, affected their mechanical and tribological properties. The nanoindentation results showed that the peak values of the hardness and the corresponding indentation depth increased along with increasing film thickness. In the scratch resistance tests, the critical load was independent of the thickness for thinner films, however, it then increased rapidly with increasing film thickness (for thicker films). Nevertheless, the critical load did not improve effectively using very thick films. It was found in ball-on-disk sliding tests that the friction coefficient decreased with increasing thickness for thinner films, but hardly decreased for relatively thick films. The decrease of the friction coefficient at the beginning of the sliding could be attributed to the formation of transferred layers from the films to the sliding balls and the graphitization of the films during sliding.

References

[1] Y. Lifshitz, Diamond Relat. Mater. 8 (1999) 1649.
[2] A. Grill, Thin Solid Films 355–356 (1999) 189.
[3] M.K. Arora, A.H. Lettington, D.R. Waterman, Diamond Relat. Mater. 8 (1999) 623.
[4] H. Boving, H. Hintermann, W. Hänni, Proc. 3rd European Space Mechanisms & Tribology Symposium, Madrid, Spain, ESA SP-196 (1987) 155.
[5] T.P. Chang, H.S. Cheng, W.A. Chiou, W.D. Sproul, Tribology Trans. 34 (1991) 408.
[6] D.F. Wang, K. Kato, Wear 223 (1998) 167.

[7] V. Hajek, K. Rusnak, J. Vlcek, L. Martinu, S.C. Gujrathi, J. Vac. Sci. Technol. A 17 (1999) 899.

[8] T.W. Scharf, H. Deng, J.A. Barnard, J. Appl. Phys. 81 (1997) 5393.

[9] E.C. Cutiongco, D. Li, Y.P. Chung, C.S. Bhatia, J. Tribol. 118 (1996) 543.

[10] M. Kohzaki, A. Matsumuro, T. Hayashi, M. Muramatsu, K. Yamaguchi, Thin Solid Films 308–309 (1997) 239.

[11] B. Wei, B. Zhang, K.E. Johnson, J. Appl. Phys. 83 (1998) 2491.

[12] N.R. Moody, D. Medlin, D. Boehme, D.P. Norwood, Eng. Fracture Mech. 61 (1998) 107.

[13] M.K. Fung, W.C. Chan, K.H. Lai, I. Bello, C.S. Lee, N.B. Wong, S.T. Lee, J. Non-Cryst. Solids. 254 (1999) 167.

[14] W.C. Oliver, G.M. Pharr, J. Mater. Res. 7 (1992) 1564.

[15] T. Sawa, Y. Akiyama, A. Shimamoto, K. Tanaka, J. Mater. Res. 14 (1999) 2228.

[16] T.Y. Tsui, G.M. Pharr, J. Mater. Res. 14 (1999) 292.

[17] X. Cai, H. Bangert, Thin Solid Films 264 (1995) 59.

[18] P.J. Burnett, D.S. Rickerby, Thin Solid Films 154 (1987) 403.

[19] P.J. Burnett, D.S. Rickerby, Thin Solid Films 157 (1988) 233.

[20] F. Attar, T. Johannesson, Surf. Coat. Technol. 78 (1996) 87.

[21] S.J. Bull, Tribol. Int. 30 (1997) 491.

[22] K. Holmberg, A. Matthews, Coatings Tribology, Elsevier Science, Amsterdam, 1994, p. 99.

[23] D.S. Kim, T.E. Fischer, B. Gallois, Surf. Coat. Technol. 49 (1991) 537.